Available online at www.sciencedirect.com
SCIENCE DIRECT®
Journal of Solid State Chemistry 177 (2004) 1165–1172
JOURNAL OF SOLID STATE CHEMISTRY
http://elsevier.com/locate/jssc

Epitaxial growth of Ag_2S films on MgO(001)

Hiroshi Nozaki,* Mitsuko Onoda, Ken Yukino, Keiji Kurashima, Kousuke Kosuda, Hideyuki Maki, and Shunichi Hishita

National Institute for Materials Science, 1-1 Namiki, Tsukuba, Ibaraki, 305-0044, Japan

Received 23 July 2003; received in revised form 21 October 2003; accepted 26 October 2003

Abstract

Epitaxial films of monoclinic Ag_2S on polished and annealed surfaces and on cleaved surfaces of MgO(001) were prepared by molecular beam epitaxy. The films were characterized by X-ray diffraction method. Ag_2S films generally consisted of crystallites with orientations of (012), (−1,1,2) and (010) parallel to substrate surfaces, but for a thick film (180 nm) on cleaved MgO, the (010) orientation was not observed. In-plane orientation of the (−1,1,2) oriented crystallites was essentially the same as that of the (012) oriented crystallites in any case. That for the (010) oriented crystallites was not determined. For a film deposited on the polished MgO substrate, in-plane orientation for (012) oriented crystallites was $[100]\|[110]_{MgO}$. For a film on the cleaved MgO substrate, the main in-plane orientation was $[100]\|[100]_{MgO}$. For the thick film on the cleaved MgO substrate, the in-plane orientation was basically $[4,-2,1]\|[100]_{MgO}$ with slight modifications. There exist additional orientations due to twinning based on the monoclinic lattice of Ag_2S in each case.

Keywords: Silver sulfide; Epitaxial films; Molecular beam epitaxy; X-ray diffraction; Magnesium oxide; Twinning

1. Introduction

Epitaxial Ag_2S films have been prepared on NaCl(001) substrates [1–3] and also on AgBr polycrystalline films by vacuum-deposition method [4]. It has been confirmed by electron diffraction measurements that Ag_2S films on NaCl(001) surfaces grow epitaxially with $[100](012)Ag_2S\|[110](001)NaCl$ [1,3,5]. The (012) orientation which is parallel to the substrate surface has been also observed for Ag_2S films deposited on AgBr(001) and those prepared by sulfurating surfaces of silver single-crystal films [6,7]. Electrical resistance, photoconduction and optical transmission of epitaxial Ag_2S film on NaCl have been reported [1]. Polycrystalline Ag_2S films have been prepared by many authors due to potential applications of semiconducting and ion conducting properties of Ag_2S [8–16].

Ag_2S films deposited on cleaved MgO(001) in our previous X-ray diffraction study showed that the films consist of crystallites with (−1,1,2) and (010) orientations, respectively, as well as the (012) orientation mentioned above [17]. This situation differs from the observation of Ag_2S films prepared on NaCl, AgBr and Ag substrates. The existence of these orientations should be naturally realized when the cubic to monoclinic transition of Ag_2S occurs at the transition temperature 177°C upon cooling [18]. Thus, the difference may be ascribed to use MgO substrates in our deposition experiments of Ag_2S films or to use X-ray diffraction for their characterization. X-ray diffraction is very sensitive to lattice periodicity normal to substrate surface, while transmission electron diffraction very sensitive to lattice periodicity perpendicular to substrate surface.

In-plane epitaxial relations of Ag_2S films on cleaved MgO(001) substrates in our previous study [17], which were dependent on film thickness, were determined by X-ray intensity measurements of some reflections by setting films at particular ϕ-positions expected at which these reflections would be observed. It did not extend overall ϕ-rotation within the substrate surface and did not give a whole aspect of the in-plane epitaxy. Therefore, it seems to be necessary to clear the whole aspect of in-plane epitaxy for Ag_2S films on MgO substrates first of all.

*Corresponding author. Fax: +81-29-852-7449.
E-mail address: nozaki.hiroshi@nims.go.jp (H. Nozaki).

0022-4596/$ - see front matter © 2003 Elsevier Inc. All rights reserved.
doi:10.1016/j.jssc.2003.10.027

We attempted to produce Ag_2S epitaxial films on polished and annealed surfaces of MgO(001) substrates and on cleaved MgO(001) substrates. The aim of the present study is to clarify the epitaxial relations of Ag_2S films on these substrates by X-ray diffraction method.

The structure of β-Ag_2S is cubic with a body centered cubic array of sulfur ions ($a = 0.4860$ nm at 186°C) [18]. That of α-Ag_2S is monoclinic with a body centered pseudocubic array of sulfur ions ($A = 0.4231$ nm, $B = 0.6930$ nm, $C = 9.526$ nm, and $\beta = 125.48°$ at room temperature) [19]. For convenience of later discussion, relations between the monoclinic and cubic lattices of α- and β-Ag_2S are given; $\mathbf{A} = 1/2(\mathbf{a} - \mathbf{b} - \mathbf{c})$, $\mathbf{B} = \mathbf{a} + \mathbf{b}$ and $\mathbf{C} = 2\mathbf{c}$. The **C**-axis was changed to be [101] for the ICDD data No. 14–72 to emphasize and clarify the understanding of the relation between monoclinic and cubic lattices of Ag_2S, as indicated in Ref. [19].

2. Experimental

Deposition experiments were carried out by molecular beam epitaxy (MBE). Our experimental setup was described in a previous work [17]. Polished substrates of MgO(001) were annealed at 1080°C in an O_2 atmosphere to obtain flat surfaces [20,21]. Substrate temperature was maintained between 270°C and 300°C during the deposition experiments.

Nominal thickness of the deposition film on the polished and annealed MgO substrate was $t = 185$ nm, where the nominal thickness here was the product of the silver deposition rate and deposition time. Silver film thickness for the deposition rate was estimated by a stylus method. Another deposition experiment, in which both cleaved and polished-annealed MgO(001) substrates were simultaneously set on a substrate holder, was also made to clarify the difference between characteristics of both films deposited on the substrates. Nominal thickness of each film was $t = 44$ nm. Thick films with nominal thickness of 180 nm on cleaved and polished MgO(001) were also prepared under the simultaneous deposition process mentioned above.

Epitaxial characteristics of the Ag_2S films were examined by an X-ray diffractometer which was equipped with line-focused Cu$K\alpha$ source and a curved incident monochrometer. The diffractometer had not a conventional divergent incident beam but a converged incident beam [22]. The diffractometer had a device to move a film toward directions parallel and vertical to the surface and rotate it around the ϕ-axis normal to the surface. The device made it possible to measure positional variation of film characteristics and ϕ-dependence of reflection intensity.

X-ray reflections for lattice planes parallel to the substrate surface were collected by $\theta - 2\theta$ scanning mode with an ordinary symmetrical arrangement of incident and reflected X-ray beam. An X-ray reflection for a lattice plane inclined relative to the substrate surface was measured by setting an appropriate angle of ϕ-rotation and an offset angle for the θ-axis (Ω rotation). The offset angle corresponded to an interplanar angle (denoted as α) between one lattice plane parallel to the substrate surface and the indicated lattice plane. The ϕ-dependence of reflection intensity of an appropriate inclined lattice plane was measured to determine in-plane epitaxy of Ag_2S film. The indicated reflection intensity was obtained from the rocking curve profile around the θ-axis.

3. Results and discussion

3.1. X-ray diffraction data

An X-ray diffraction pattern in $\theta - 2\theta$ scanning mode for a Ag_2S film on a substrate of MgO(001) is shown in Fig. 1. Reflections marked by * in the figures result from substrates; they include reflections due to $\lambda/2$ and $\lambda/3$ as well as λ, the wavelength of Cu$K\alpha$. The pattern indicates that lattice planes of Ag_2S parallel to the substrate surface are (−1,1,2) and (012) within an angle of 0.1° at most. These lattice planes together with (020) correspond to $\{110\}_c$ of the high-temperature cubic form, i.e., the lattice planes most dense in the sulfur packing of body-centered lattice. The reflection of 040 was not seen at $2\theta = 52.9°$ in Fig. 1, where an optimum offset angle was set for 0 0 2 reflection of MgO substrate. However, the reflection of 0 4 0 was observed in Table 1, as mentioned later, by setting an optimum offset angle for this reflection. Thus, (010) orientation also exists as a minor one, compared with the (−1,1,2) and (012) orientations.

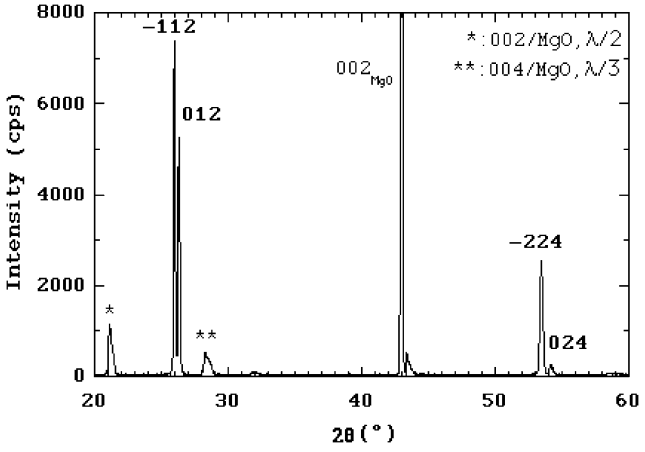

Fig. 1. X-ray diffraction pattern of Ag_2S film on polished MgO with $\theta - 2\theta$ scanning mode. Reflections marked by * are those due to the substrate. Intensity of MgO 0 0 2 reflection is reduced.

Table 1
Observed and calculated d spacing and interplanar angles; observed intensity for Ag_2S films on polished MgO(001)

$h\,k\,l$	d_{obs} (nm)	d_{cal} (nm)	α_{obs} (deg)	α_{cal} (deg)	I_{obs} (%)
−1 1 2	0.34352	0.34292	0.0	0.0	100
	0.34409	0.34401	0.1	0.0	18
0 1 2	0.33854	0.33860	0.0	0.0	98
	0.33877	0.33855	0.1	0.0	100
0 1 3	0.24276	0.24245	8.7	8.8	14
	0.24232	0.24233	8.8	8.8	15
0 2 3	0.20728	0.20725	7.4	7.5	5
	0.20731	0.20728	7.5	7.5	5
0 1 4	0.18701	0.18693	13.5	13.6	3
	0.18677	0.18681	13.7	13.6	4
0 4 0	0.17299	0.17294	0.1	0.0	<1
	0.17329	0.17328	0.1	0.0	5
−2 2 4	0.17157	0.17146	0.0	0.0	9
	0.17196	0.17200	0.1	0.0	7
0 2 4	0.16897	0.16930	0.0	0.0	6
	0.16928	0.16927	0.1	0.0	6
−2 3 2	0.15464	0.15465	26.2	27.2	<1
	0.15391	0.15391	26.8	27.0	1
0 1 5	—	0.15155	—	16.7	—
	0.15142	0.15144	16.7	16.6	2
−2 1 6	0.15134	0.15134	25.7	26.6	<1
	—	0.15279	—	26.8	—
0 6 0	—	0.11529	—	0.0	—
	0.11550	0.11552	0.1	0.0	1
0 3 6	—	0.11287	—	0.0	—
	0.11280	0.11285	0.1	0.0	1

$A = 0.4225$ nm, $B = 0.6918$ nm, $C = 0.9512$ nm, and $\beta = 125.27°$ for Film1 (upper columns).
$A = 0.4201$ nm, $B = 0.6931$ nm, $C = 0.9611$ nm, and $b = 126.16°$ for Film2 (lower columns).

Table 2
Observed and calculated d spacing and interplanar angles; observed intensity for Ag_2S films on cleaved MgO(001)

$h\,k\,l$	d_{obs} (nm)	d_{cal} (nm)	α_{obs} (deg)	α_{cal} (deg)	I_{obs} (%)
−1 1 2	0.34346	0.34332	0.0	0.0	28
	0.34407	0.34457	0.0	0.0	100
0 1 2	0.33820	0.33815	0.0	0.0	100
	0.33871	0.33867	0.0	0.0	34
0 1 3	0.24179	0.24205	8.6	8.8	13
	—	0.24274	—	8.7	—
0 2 3	0.20700	0.20703	7.3	7.5	5
	—	0.20696	—	7.4	—
0 1 4	0.18683	0.18660	13.3	13.6	3
	—	0.18726	—	13.7	—
0 4 0	0.17303	0.17003	0.0	0.0	6
	—	0.17148	—	0.0	—
−2 2 4	0.17164	0.17166	0.0	0.0	6
	0.17180	0.17228	0.0	0.0	14
−2 3 2	0.15482	0.15483	26.2	27.2	<1
	0.15553	0.15456	26.1	27.1	2
1 3 2	—	0.15336	—	26.5	—
	0.15272	0.15295	26.3	26.3	1
0 1 5	0.15118	0.15127	16.5	16.6	<1
	—	0.15186	—	16.7	—
−1 1 6	—	0.15000	—	25.9	—
	0.15142	0.15102	25.7	26.0	1
0 6 0	0.11536	0.11535	0.0	0.0	1
	—	0.11432	—	0.0	—
−3 3 6	0.11441	0.11444	0.0	0.0	<1
	—	0.11487	—	0.0	—
0 3 6	0.11277	0.11272	0.0	0.0	1
	—	0.11286	—	0.0	—
−3 4 4	—	0.10934	—	18.9	—
	0.10917	0.10930	18.8	18.8	2
1 4 4	—	0.10797	—	18.3	—
	0.10769	0.10779	18.5	18.2	<1

$A = 0.4233$ nm, $B = 0.6921$ nm, $C = 0.9506$ nm, and $\beta = 125.4°$ for Film3 (upper columns).
$A = 0.4256$ nm, $B = 0.6859$ nm, $C = 0.9588$ nm, and $b = 125.7°$ for Film4 (lower columns).

The X-ray reflections observed for two Ag_2S films on polished MgO(001) substrates are listed in Table 1. Both films whose data are listed in the upper and lower sites in the columns of Table 1 were named as Film1 ($t = 185$ nm) and Film2 ($t = 44$ nm), respectively. In the table, α_{obs} for each reflection is an observed interplanar angle between the indicated lattice plane and the lattice plane parallel to the substrate surface, and α_{cal} is calculated one. Interplaner angles were used to specify indices of the lattice planes observed. Lattice parameters obtained by the least-squares method are also shown there. Reflections listed in Tables 1 and 2 were measured with the most optimum offset angle around θ-axis for each reflection.

X-ray reflections observed for Ag_2S films (Film3 (44 nm) and Film4 (180 nm)) on the cleaved surface of MgO(001) are also listed in Table 2. The specimens, Film3 and Film2, were simultaneously deposited under the same experimental conditions except substrate surface states. X-ray patterns in Fig. 1 are produced by specimen of Film1.

The specimen, Film2, was freshly prepared for measurements of ϕ-dependence of reflection intensity, as mentioned in later sections, because profiles of the ϕ-dependence for the specimen Film1 was broadened, probably due to a long period (about 1 year) after preparation. Obviously, however, X-ray pattern of Film2 included 111 and 222 reflections of silver, while the X-ray pattern of film3 on the cleaved MgO substrate, which was simultaneously prepared with Film2, did not include these reflections. This suggests that sulfur behavior may be different on cleaved and polished surfaces of MgO.

Thick films (180 nm) on cleaved and polished MgO surfaces were also prepared by simultaneous deposition to confirm previous results of in-plane epitaxy [17]. The X-ray reflection data of thick film (Film4) on cleaved MgO substrate are also listed in Table 2. In contrast with this thick film on the cleaved MgO substrate, the thick film on polished MgO substrate gave no reflection pattern of Ag_2S, but an amorphous-like reflection pattern, which was different from the case of Film1 with almost the same thickness.

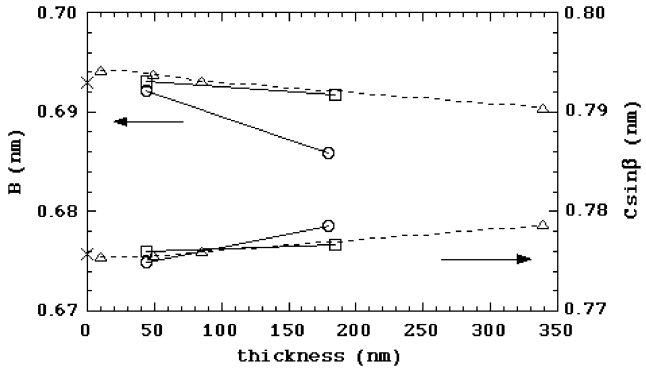

Fig. 2. Thickness dependence of lattice dimensions, B and $C\sin\beta$. Squares and circles on solid lines indicate data of the present films on polished and cleaved MgO substrate, respectively. Triangles on dotted lines indicate previous data of a film on cleaved MgO.

The lattice dimensions obtained are dependent on film thickness. Thickness dependences of B and $C\sin\beta$ are shown in Fig. 2 for comparison with previous data [17]. The thickness dependence of the present dimensions are similar to the previous data, i.e., B decreases with increasing thickness, while $C\sin\beta$ increases. The magnitudes of B and $C\sin b$ at 44 nm in the abscissa are almost the same as that of bulk [18]. The decrease of B for Film4 is rather larger than that of previous B. The elongation of $C\sin\beta$, which is elongation along the direction perpendicular to **A** within (010), is associated with the contraction of **B** whose direction is perpendicular to (010). These dependences may suggest that distortion of Ag_2S films increases with film thickness.

3.2. Intensity profile for ϕ-rotation

3.2.1. Film on polished MgO substrate

Many reflections $0\,k\,l$'s are recorded in Table 1. The ϕ-dependence of intensity of any $0\,k\,l$ except 0 1 2 gives the direction of **A** [100], which is parallel to the substrate surface, because **A** is parallel to any ($0kl$) together with (012). The ϕ-dependence of intensity of 0 1 5 for Film2 was measured to determine the in-plane epitaxy of crystallites with the (012) orientation. It is shown in Fig. 3, where intensities of 333 and its equivalents for MgO are also plotted with their peak positions which specify $\langle 110\rangle$ of the MgO substrate. Main peak positions of the 0 1 5 profile are at about 45°, 135°, 225°, etc.; satellite peak positions are at about 6°, 25°, 65°, 84°, etc., where the peak profile is nearly symmetric around $\langle 110\rangle$ of MgO.

The ϕ-dependence of intensity of $-2,3,2$ might yield in-plane epitaxy of crystallites with the $(-1,1,2)$ orientation, as shown later in Section 3.2.2. The reflection of $-2,3,2$ was observed with maximum intensity at about $\phi = 110°$, but its ϕ-dependence was not investigated because of weak intensity.

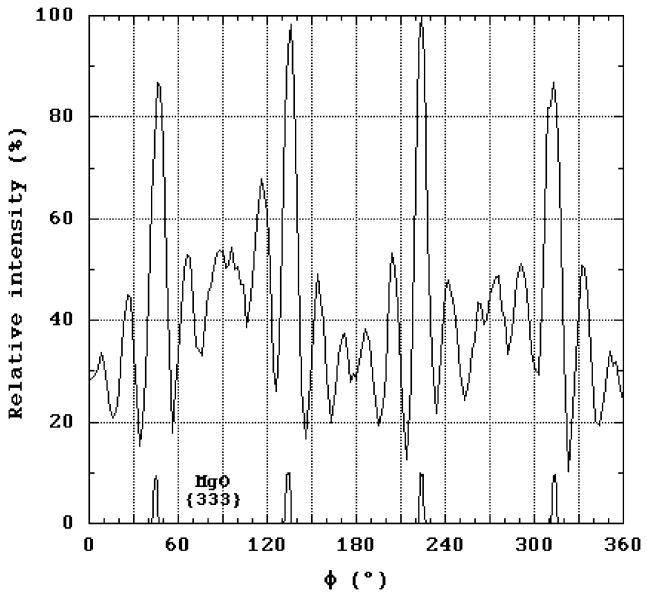

Fig. 3. ϕ-Dependence of reflection intensity of 0 1 5 for a film on polished MgO together with that of 333 for the MgO substrate.

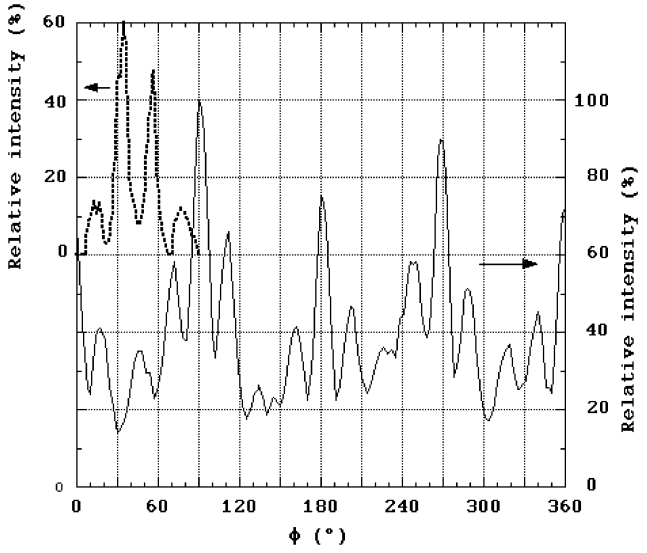

Fig. 4. ϕ-Dependence of reflection intensity of 0 1 5 for a film on cleaved MgO (solid curve) and that of $-2\,3\,2$ (dotted curve).

3.2.2. Film on cleaved MgO substrate

The ϕ-dependence of intensity of 0 1 5 for Film3 is shown by a solid curve in Fig. 4, where directions [100] and [010] of MgO correspond to 0° and 90°, respectively. Main peak positions were observed at about 0°, 90°, 180°, etc. and satellite peak positions were done at about 20°, 70°, 110°, etc., where weak additional peaks were further observed at 45°, 135°, 225° and 315°. The profile of the ϕ-dependence is symmetric around $\langle 100\rangle$ of MgO.

The ϕ-dependence of intensity of $-2,3,2$ is shown by a dotted curve in Fig. 4. Main peak positions are seen at 35° and 55°; satellite peak positions are done at about 12° and 77°.

3.2.3. Thick film on cleaved MgO substrate

Our previous study showed that in-plane epitaxy of Ag_2S thick film (>80 nm) differs from that of Ag_2S thin film in the use of cleaved MgO(001) substrates [17]. To confirm this result, the ϕ-dependence of intensity of 1 4 4 for Film4 is shown in Fig. 5, where directions [100] and [010] of the MgO substrate correspond to 0° and 90° in the abscissa, respectively. Notably, (144) and (012) are parallel to $\mathbf{A}-1/2\mathbf{B}+1/4\mathbf{C}$, that corresponds to the cubic lattice vector $-\mathbf{b}$, so that the ϕ-dependence of intensity of 1 4 4 indicates the direction of $\mathbf{A}-1/2\mathbf{B}+1/4\mathbf{C}$ within the plane of substrate surface, which gives the in-plane epitaxy of crystallites with the (012) orientation.

The ϕ-dependence of intensity of $-3\,4\,4$ was also measured to clarify in-plane epitaxy of crystallites with (−1,1,2) orientation. Fig. 6 clarifies the similarity of results with that for the (012) orientation.

3.3. Epitaxial relations

The Ag_2S films on several substrates show that lattice planes {012}, {−1,1,2} and {010} are parallel to substrate surfaces within 0.1° at most, i.e., the (012) (−1,1,2) and (010) orientations; the former two orientations are major ones. In contrast with the orientation parallel to the substrate surface, in-plane epitaxy of the films vary according to the type of substrate and the film thickness. Moreover, the profile of ϕ-dependence of reflection intensity is also complex due to presence of twinning.

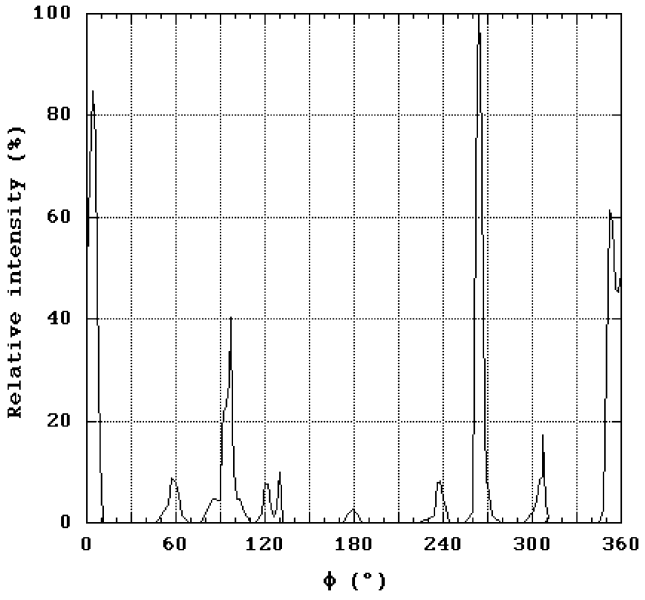

Fig. 5. ϕ-Dependence of intensity of $-3\,4\,4$ for a thick film on cleaved MgO.

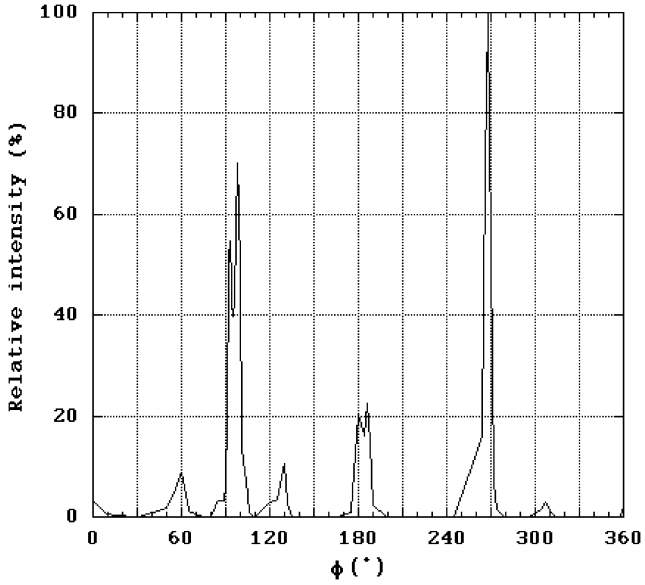

Fig. 6. ϕ-Dependence of intensity of 1 4 4 for a thick film on cleaved MgO.

Some twinning relations are supposed to explain ϕ-dependence of reflection intensity. In the inset of Fig. 7, illustration of (012) oriented and (0,−1,2) oriented crystallites are given, where (1,−2,0) and (120) together with (3,0,−4) are candidates of twinning planes. Since angles of (012) with (1,−2,0) and (3,0,−4) are very close to 90° and those of (0,−1,2) with (12 0) and (3,0,−4) are also very close to 90°, (012) and (0,−1,2) oriented crystallites can overlap with small misfit angles across (1,−2,0) and (120) or (3,0,−4). For (−1,1,2) and (−1,−1,2) oriented crystallites, (120) and (1,−2,0) or (104) could be twinning planes. In Fig. 7, both (012) crystallite (shown by dotted rectangle) and (0,−1,2) crystallite (open one) are adjacent by overlap of twinning planes, (1,−2,0) and (120), where solid arrows indicate 2**A**. Another twinning relation between (012) and (0,−1,2) crystallites is represented by a mirror plane (3,0,−4), represented by dotted lines. These twinning relations were used to explain ϕ-dependence of reflection intensity.

3.3.1. In-plane epitaxy of Ag_2S on polished MgO(001)

In-plane epitaxial relations of Ag_2S on the substrate of polished MgO(001), based on the result of Fig. 3 and the twin relations mentioned above, are illustrated in Fig. 7: 2**A** for crystallites bearing the main in-plane epitaxy is depicted so as to be parallel to $\langle 110\rangle_{MgO}$. A dotted line indicates the twinning plane of (3,0,−4) for the (012) orientation crystallites. The twinning plane for

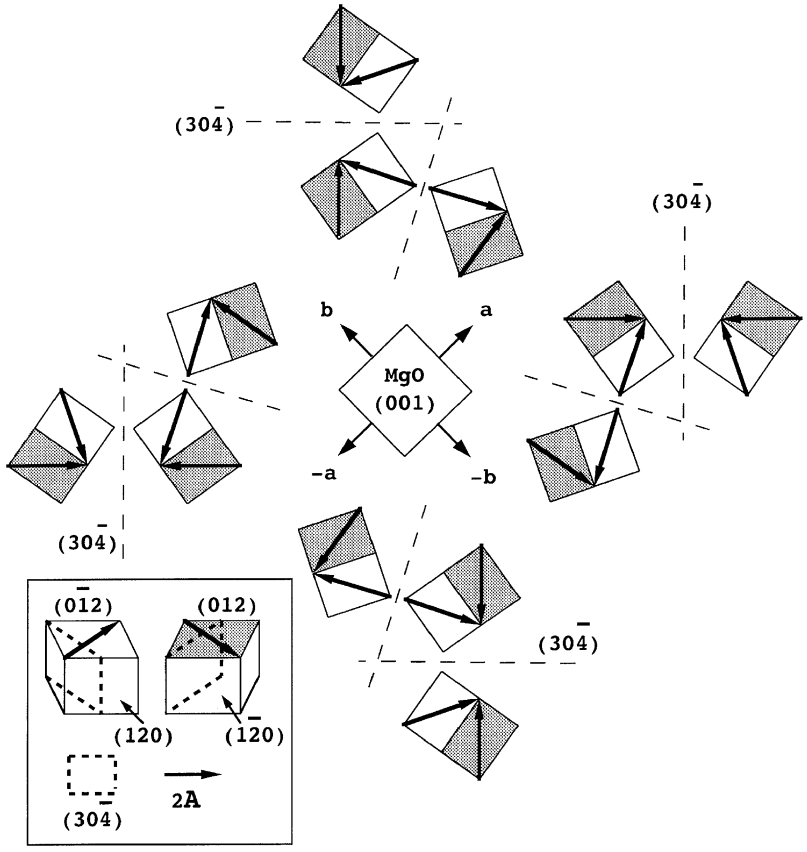

Fig. 7. Illustration of in-plane epitaxy of a film deposited on polished MgO(001). Solid arrows and dotted lines represent 2**A** and twinning planes (3,0,−4), respectively. Illustration of the inset shows twinning planes, (1,−2,0), (1,2,0) and (3,0,−4), supposed for twinning between (012) and (0,−1,2) oriented crystallites, represented by dotted and open rectangles, respectively.

the (−1,1,2) orientation crystallites is (104). In-plane epitaxy in the illustration gives peak positions of the ϕ-dependence of intensity of 015, such as 5.1°, 25.0°, 45.0°, 65.0°, etc., which are in good agreement with experimental results. Thus, the main in-plane epitaxy of Ag_2S on polished MgO(001) is

$$\mathbf{A}\|[110]_{MgO}$$

followed by additional orientations of in-plane epitaxy caused by the twinning.

The in-plane epitaxy for (−1,1,2) oriented crystallites may be identified to that for (012) oriented crystallites because: (1) both crystallites are equivalent in the high-temperature cubic phase; (2) their in-plane lattice dimensions are almost identical to each other because of the small distortion of monoclinic lattice from the cubic symmetry; and (3) the reflection of −2 3 2 was observed at $\phi = 100°$. The last reason strongly supports the above statement that in-plane epitaxy of the (−1,1,2) oriented crystallites is the same as that of the (012) oriented crystallites because the peak positions of ϕ-dependence of −2 3 2 are estimated from the lattice dimensions of Film2 to be at 10°, 80°, and 100°, etc. This is true for reason in the next section describing the angle between $\mathbf{A} + 1/2\mathbf{C}$ and $\mathbf{A} + 1/2\mathbf{B} + 1/4\mathbf{C}$ (55.0° for this case).

The epitaxial relation of Film2, [100](012) $Ag_2S\|[110](001)MgO$ is the same as that of Ag_2S film on NaCl substrate [3], but their relation between the lattice periodicity of film and substrate is quite different. Interplanar distance of NaCl along [110] is 0.399 nm which almost agrees with lattice dimension A of Ag_2S, which may cause the epitaxial relation reported [3,5], while that of MgO is 0.298 nm. One explanation for the present case is that a rhomb which consists of sulfur ions at the origin, 2**A**, i.e., $[1,-1,-1]_c$, and $-\mathbf{B} + 1/2\mathbf{C}$, i.e., $[-1,-1,1]_c$, within (012), i.e., $(101)_c$, almost agrees with a parallelogram which consists of Mg ions at the origin, $3/2(\mathbf{a}_{MgO} + \mathbf{b}_{MgO})$ and $\mathbf{a}_{MgO} - 2\mathbf{b}_{MgO}$ within substrate surface ($a_{MgO} = 0.4213$ nm). Dimensions of 2**A** (0.840 nm) and $\mathbf{B} + 1/2\mathbf{C}$ (0.843 nm) are 6.0% and 10.5% smaller than dimensions of $3/2(\mathbf{a}_{MgO} + \mathbf{b}_{MgO})$ and $\mathbf{a}_{MgO} - 2\mathbf{b}_{MgO}$, respectively. The angle between 2**A** and $-\mathbf{B} + 1/2\mathbf{C}$ (109.66°) is 1.1% larger than that between $3/2(\mathbf{a}_{MgO} + \mathbf{b}_{MgO})$ and $(\mathbf{a}_{Mgo} - 2\mathbf{b}_{MgO})$. The almost agreement between the rhomb and parallelogram may cause the in-plane epitaxy observed.

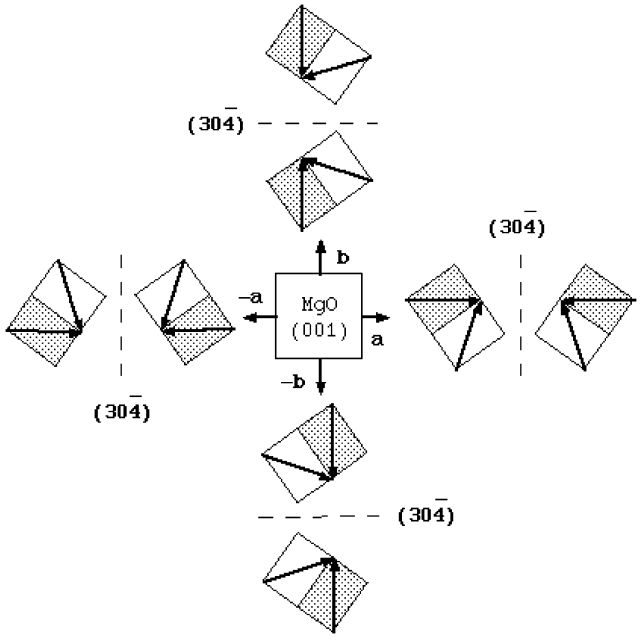

Fig. 8. Illustration of in-plane epitaxy of a film deposited on cleaved MgO(001). Solid arrows and dotted lines represent 2**A** and twinning planes.

3.3.2. *In-plane epitaxy of Ag_2S on cleaved MgO(001)*

In-plane epitaxial relations of Ag_2S on the substrate of cleaved MgO(001), based on the result of Fig. 4 and the discussion of twinning planes, are shown in Fig. 8: **A** is parallel to $\langle 100 \rangle_{MgO}$ and (30−4) and (1−20) are also twinning planes for the (012) oriented crystallites. The illustration of in-plane epitaxy in the figure shows peak positions of ϕ-dependence of intensity of 0 1 5, such as 0.0°, 20.0°, 70.0°, 90.0°, etc., which agree well with experimental results except for the lack of peak positions at 45°, 135°, 225°, and 315° as shown in Fig. 8. Weak peaks at these positions are observed as main peaks in Fig. 3. These peaks may be ascribed to slight presence of in-plane epitaxy like that of Film2. Thus, the main in-plane epitaxy of the (012) oriented crystallites for thin Ag_2S film on cleaved MgO(001) is

$$\mathbf{A} \| [100]_{MgO}$$

following the additional orientations of in-plane epitaxy caused by the twinning. The orientation of $\mathbf{A}//[110]_{MgO}$ is also present but minor, as shown by weak peaks at 45° and 315° in Fig. 4.

In-plane epitaxy of the (−112) oriented crystallites is shown in Fig. 8, except that 2**A** (solid arrow) should be replaced by $2\mathbf{A}+\mathbf{C}$, where 2**A** and $2\mathbf{A}+\mathbf{C}$ correspond to $[1,-1,-1]_c$ and $[1,-1,1]_c$ of the high-temperature cubic lattice, respectively. A twinning plane (3,0,−4) in the figure should be also replaced by the one (104). Since the vector $\mathbf{A}+1/2\mathbf{B}+1/4\mathbf{C}$ (cubic lattice vector **a**), as mentioned in the section of 3.3.1, is at 54.6° with $\mathbf{A}+1/2\mathbf{C}$ within (−1,1,2), the ϕ-dependence of intensity of $-2,3,2$ based on the illustration shows peak positions 35.4° and 54.6° which agree with the experimental observation. Further, additional orientations like $\mathbf{A}+1/2\mathbf{C}//[110]_{MgO}$ yield peak positions 9.6° and 80.4°. These values differ slightly from experimental values of 12° and 77°, which may be ascribed to inaccuracy in measurements of very weak reflection.

The main in-plane epitaxy agrees with a previous study for thin films ($t<50$ nm) on cleaved MgO(001) substrates [17], where it was pointed out that the length of **A** well agrees with that of lattice dimension for the MgO substrate. If one can consider a rhomb which consists of the origin, **A**, $(1/2[1,-1,-1]_c)$, and $-1/2\mathbf{B}+1/4\mathbf{C}$, $(1/2[-1,-1,1]_c)$, within (012), $((101)_c)$, a parallelogram which consists of sulfur ions at the origin, **A** and $3(-1/2\mathbf{B}+1/4\mathbf{C})$ almost agrees with that which consists of Mg ions at the origin, $\mathbf{a}_{MgO}(\mathbf{a}_{MgO}\|\mathbf{A})$ and $-\mathbf{a}_{MgO}-3\mathbf{b}_{MgO}$ within the substrate surface. Dimension of **A** is 0.5% larger than that of $\mathbf{a}_{MgO}$ and dimension of $3(-1/2\mathbf{B}+1/4\mathbf{C})$ 5.5% smaller than that of $-\mathbf{a}_{MgO}-3\mathbf{b}_{MgO}$. The relations of angles of these vectors are the same as those in Section 3.3.1. In addition, with the almost agreement between the in-plane periodicity of the film and substrate, steps caused upon cleavage may play a role in the in-plane epitaxy of the film on cleaved MgO substrate because this in-plane epitaxy differs with that of the film on polished and annealed MgO substrate which has no steps comparable with heights of Ag_2S crystallites. Although main in-plane epitaxy differs from that of the polished MgO substrate, in-plane epitaxy such as that observed for Film2 is present as a minor one. This fact may suggest that energy difference is small between both in-plane epitaxies of films on the cleaved and polished MgO substrates.

3.3.3. *In-plane epitaxy of Ag_2S thick film on cleaved MgO(001)*

In-plane epitaxy of a thick film (180 nm) on the cleaved MgO(001) substrate indicates that $\mathbf{A}-1/2\mathbf{B}+1/4\mathbf{C}$ for (012) oriented crystallites and $\mathbf{A}+1/2\mathbf{B}+1/4\mathbf{C}$ for (−1,1,2) oriented crystallites are nearly parallel to $\langle 100 \rangle_{MgO}$, accompanying the minor orientations of $\mathbf{A}//\langle 010 \rangle_{MgO}$ for the (012) oriented crystallites and $\mathbf{A}+1/2\mathbf{C}//\langle 010 \rangle_{MgO}$ for the (−1,1,2) orientated crystallites, respectively. Minor orientations of the thick film are similar to those observed for the thin film on the cleaved MgO(001) substrate. These facts agree with previously reported results [17]. It was pointed out in Ref. [17] that in-plane epitaxy of thick film ($t>800$ μm) is strongly affected by existence of steps on the cleaved MgO surface, which changes the in-plane orientation and size of crystallites to the present orientation and large size of crystallites of

about 100 μm order in length. However, the present study indicates some modifications such as presence of splits of peak profiles in ϕ-dependence of intensity of 144 and that of intensity of -344, as shown in Figs. 5 and 6. Although these splits may be caused by monoclinic distortion of Ag_2S, details remain unknown.

4. Conclusion

Ag_2S epitaxial films were prepared on polished and cleaved MgO(001) substrates by MBE. Epitaxial relations between films and substrates were determined by an X-ray diffraction method.

For a film ($t = 44$ nm) on polished MgO, [100](012)Ag_2S‖[110](001)MgO and [201](−1,1,2) Ag_2S‖[110](001)MgO.

For a film ($t = 44$ nm) on cleaved MgO, [100](012)Ag_2S‖[100](001)MgO and [201](−1,1,2) Ag_2S‖[100](001)MgO.

For a thick film ($t = 180$nm) on cleaved MgO, [4,−2,1](012)Ag_2S‖[100](001)MgO and [4,2,1](−1,1,2) Ag_2S‖[100](001)MgO.

In addition, with each main orientation described above, there are always satellite orientations due to twinning. In-plane epitaxy of (010) oriented crystallites was not determined because of their minor existence.

Acknowledgments

The authors would like to thank Dr. S. Aizawa (NIMS) for his advice in the experiment of reflection high-energy electron diffraction. Appreciation is also offered to Dr. H. Wada and Dr. E. Takayama-Muromachi (NIMS) for their encouragement of this work.

References

[1] A. Ichimescu, U. Constatinescu, Rev. Roum. Phys. 17 (1972) 163–167.
[2] A. Ichimescu, G. Teodorescu, Rev. Roum. Phys. 21 (1976) 901–905.
[3] H. Haefke, A. Panov, V. Dimov, Thin Solid Films 188 (1990) 133–142.
[4] H. Haefke, H. Hofmeister, M. Krohn, A. Panov, J. Imag. Sci. 35 (1991) 164–169.
[5] K. Bozhilov, V. Dimov, A. Panov, H. Haefke, Thin Solid Films 190 (1990) 129–138.
[6] V.A. Phillips, J. Appl. Phys. 33 (1962) 712–717.
[7] M. Shiojiri, S. Maeda, Y. Murata, Jpn. J. Appl. Phys. 8 (1969) 24–31.
[8] A.J. Varkey, Sol. Energy Mater. 21 (1991) 291–296.
[9] S.S. Dhumure, C.D. Lokhande, Sol. Energy Mater. Sol. Cells 28 (1992) 159–166.
[10] M. Ristova, P. Toshev, Thin Solid Films 216 (1992) 274–278.
[11] S.S. Dhumure, C.D. Lokhande, Solar Energy Mater. Sol. Cells 29 (1993) 183–194.
[12] S. Kitova, J. Eneva, A. Panov, H. Haefke, J. Imag. Sci. Technol. 38 (1994) 484–488.
[13] A.B. Kulkarni, M.D. Uplane, C.D. Lokhande, Mater. Chem. Phys. 41 (1995) 75–78.
[14] H. Meherzi-Maghraoui, M. Dachraoui, S. Belgacem, K.D. Buhre, R. Kunst, P. Cowache, D. Lincot, Thin Solid Films. 288 (1996) 217–223.
[15] M. Amlouk, N. Brunet, B. Cros, S. Belgacem, D. Baejon, J. Phys. III 7 (1997) 1741–1753.
[16] H. Dlala, M. Amlouk, S. Belgacem, P. Girard, D. Barjon, Eur. Phys. J. Appl. Phys. 2 (1998) 13–16.
[17] H. Nozaki, M. Onoda, K. Kurashima, T. Yao, J. Solid State Chem. 157 (2001) 86–93.
[18] R.J. Cava, F. Reidinger, B.J. Wuensch, J. Solid State Chem. 31 (1980) 69–80.
[19] R. Sadanaga, S. Sueno, Miner. J. 5 (1967) 124–143.
[20] S. Kim, S. Baik, J. Vac. Sci. Technol. 13A (1995) 95–100.
[21] L.W. Guo, T. Hanada, H.J. Ko, Y.F. Chen, H. Makino, T. Yao, Surf. Sci. 445 (2000) 151–158.
[22] K. Yukino, F.P. Okamura, H. Nozaki, Y. Kobayashi, Y. Yamada, Advances in X-ray Analysis, in: C.S. Barret, et al. (Eds.), Proceedings of the Combined First Pacific-International Congress on X-ray Analytical Methods (PICXAM) and Fortieth Annual Conference on Applications of X-ray Analysis, Hiro and Honolulu, Hawaii, August 7–16, 1991, Vol. 35B, Plenum Press, New York, 1992, pp. 1275–1283.